

Measurement of absolute CO number densities in CH₃F/O₂ plasmas by optical emission self-actinometry

Erdinc Karakas¹, Sanbir Kaler, Qiaowei Lou, Vincent M Donnelly and Demetre J Economou

Plasma Processing Laboratory, Department of Chemical and Biomolecular Engineering, University of Houston, Houston, TX 77204-4004, USA

E-mail: vmdonnelly@uh.edu and economou@uh.edu

Received 22 October 2013, revised 18 December 2013

Accepted for publication 13 January 2014

Published 7 February 2014

Abstract

CH₃F/O₂ inductively coupled plasmas at 10 mTorr were investigated using optical emission spectroscopy. A ‘self-actinometry’ method was developed to measure the absolute number density of CO that formed in reactions following dissociation of CH₃F and O₂ in the plasma. In this method, small amounts of CO were added to the plasma, leading to small increases in the CO emission intensity. By carefully accounting for small perturbations to the plasma electron density and/or electron energy distribution, and by showing that very little of the CO added to the plasma was decomposed by electron impact or other reactions, it was possible to derive absolute number densities for the CO content of the plasma. With equal fractions (0.50) of CH₃F and O₂ in the feed gas, the CO mole fraction as a function of plasma power saturated at a value of 0.20–0.25. As O₂ in the feed gas was varied at a constant power of 100 W, the CO mole fraction went through a maximum of about 0.25 near an O₂ feed gas fraction of 0.5. The relative CO number densities determined by ‘standard’ actinometry followed the same functional dependence as the absolute mole fractions determined by self-actinometry, aided by the fact that electron temperature did not change appreciably with power or feed gas composition.

Keywords: plasma diagnostics, actinometry, CH₃F/O₂ plasma

(Some figures may appear in colour only in the online journal)

1. Introduction

Selective etching of silicon nitride (SiN_x) in CH₃F/O₂ plasmas has become important in integrated circuit manufacturing for forming gate spacers in field-effect transistors (FETs), including FinFETs [1]. Substrate penetration must be minimized during the over-etch period when bare silicon adjacent to the spacers is exposed to the plasma. Over-etching of the Si underneath the SiN_x spacer causes an undesirable recess in gate electrodes. As technology nodes keep shrinking, SiN_x etching selectivity over Si or SiO₂ becomes more important than ever. While etching with CH₃F/O₂ plasmas has been partially successful, the requirement for even higher selectivity remains a critical issue.

¹ Present address: GLOBALFOUNDRIES, Malta, NY, USA.

We previously reported diagnostic studies [2, 3] of CH₃F/O₂ plasmas. Langmuir probe analysis was used to measure the electron energy probability functions and electron number densities, and optical emission spectroscopy (OES) with actinometry was employed to determine relative and sometimes absolute species number densities. CO emission was one of the most intense features in the spectrum. Intense emission from OH and CO₂⁺ was also observed, hence it was not possible to determine which oxygen-containing species was the major product of plasma reactions. In those studies, no absolute calibration of CO was carried out. In the present work, an OES method for measuring absolute CO number densities was developed, using a ‘self-actinometry’ procedure similar to that reported previously for determining absolute number densities of N₂ in ammonia plasmas [4]. In that study, small

amounts of N₂ were added to the NH₃-containing plasma, leading to an increase in the N₂(C³Π_u → B³Π_g) optical emission intensity as a function of N₂ addition. This provided a calibration for obtaining the absolute N₂ number density from the relative emission intensity. It was assumed that the added N₂ was not dissociated by the plasma because of its strong bond energy, combined with the low plasma electron temperature. It was also shown that the small amount of added N₂ did not perturb the plasma, as indicated by a lack of change in Ar emission intensity.

In the present study, small known amounts of CO were added to the plasma and the resulting small increase in CO(b³Σ⁺ → a³Π) emission was recorded. Simultaneously, a small decrease in Ar emission, caused by slight changes in plasma density and/or electron energy, was observed. By showing that no detectable decomposition of the added CO occurred, the total CO emission intensity was related directly to the absolute CO number density. With this method, absolute number densities of CO as a function of power and added O₂ percentage in the CH₃F/O₂ feed gas were obtained. CO was found to be the main carbon-containing species, accounting for about a quarter of the gas in the plasma at modest to high powers.

2. Experimental procedures

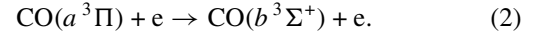
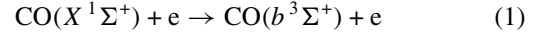
The compact inductively coupled plasma reactor used in the present study was described in previous publications [2, 3]. It consisted of a cooled (DI water at 20°C) alumina tube (inside radius $R = 1.8$ cm) surrounded by a water-cooled coil (3-turn, 1/4" OD copper tubing). Plasma formed over a length $L \approx 16$ cm. Radio frequency (13.56 MHz) power in the range of 40–400 W (0.25–2.5 W cm⁻³) was delivered to the coil. The feed gas consisting of CH₃F and O₂ was kept at a total flow rate of 10 sccm. To this flow was added a small flow of CO (0.1–1.0 sccm). A throttle valve above the turbomolecular pump was adjusted to obtain the desired pressure of 10 mTorr with no CO flow and the plasma on. This valve position was kept fixed when CO was added, hence the total pressure rose some, but the partial pressures and number densities of other species in the plasma remained nearly constant. Immediately after the plasma was extinguished, the pressure dropped by about 20% at 100 W and 35% at 300 W. For one set of experiments, Ar (0.5 sccm) was added to the flow of CH₃F (4.75 sccm) and O₂ (4.75 sccm) keeping the total flow at 10 sccm (without CO addition).

Optical emission spectra were recorded with two spectrometers (Ocean Optics model HR4000 with 1.7 Å resolution) covering the wavelength ranges of 200–427 nm and 734–916 nm. (Note that in prior publications, the lower wavelength was incorrectly given as 764 nm, not 734 nm [2, 3].) Line-averaged light emitted along the axis of the cylindrical discharge tube passed through coloured glass order sorting filters (for the 734–916 nm region) and entered the entrance slit of the spectrometer without any intervening lenses or optical fibre [2, 3]. Measurements were made as a function of small additions of CO for different powers and CH₃F:O₂ flow ratios.

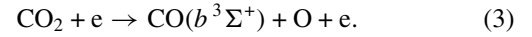
3. Results and discussion

3.1. CO Self-actinometry method

The emitting state, CO(b³Σ⁺), can be formed by electron-impact excitation of ground state CO, as well as through electron-impact excitation of the metastable CO(a³Π) state



CO(b³Σ⁺) can also be formed through dissociative excitation of a CO-containing species. The most reasonable dissociative excitation precursor is CO₂.



The relative importance of reactions (1), (2) and (3) in producing CO (b³Σ⁺ → a³Π) emission of intensities I_1 , I_2 and I_3 , respectively, can be found using the expressions

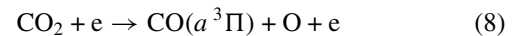
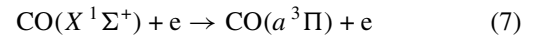
$$I_1 = \alpha n_e n_{\text{CO}} \sqrt{\frac{2e}{m_e}} \int_0^\infty \sigma_1(\varepsilon) \varepsilon^{1/2} g_e(\varepsilon) d\varepsilon = \alpha n_e n_{\text{CO}} k_1(T_e) \quad (4)$$

$$I_2 = \alpha n_e n_{\text{CO}(a)} \sqrt{\frac{2e}{m_e}} \int_0^\infty \sigma_2(\varepsilon) \varepsilon^{1/2} g_e(\varepsilon) d\varepsilon = \alpha n_e n_{\text{CO}(a)} k_2(T_e) \quad (5)$$

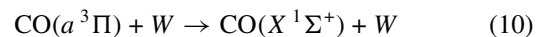
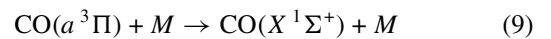
$$I_3 = \alpha n_e n_{\text{CO}_2} \sqrt{\frac{2e}{m_e}} \int_0^\infty \sigma_3(\varepsilon) \varepsilon^{1/2} g_e(\varepsilon) d\varepsilon = \alpha n_e n_{\text{CO}_2} k_3(T_e) \quad (6)$$

where α is a proportionality constant that includes light collection efficiency, detector sensitivity, Franck–Condon factors, etc, e is the elementary charge, m_e is the electron mass, n_{CO} , $n_{\text{CO}(a)}$ and n_{CO_2} are the number densities of CO ground state, CO(a³Π) and CO₂, respectively, $\sigma_i(\varepsilon)$ and $k_i(T_e)$ ($i = 1, 2, 3$) are the electron-impact cross sections and rate coefficients for reactions (1)–(3), ε is the electron energy, $g_e(\varepsilon)$ is the electron energy distribution function (EEDF), and T_e is the electron temperature for the near-Maxwellian EEDF that is found for this system below ~20 mTorr [3].

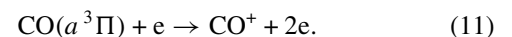
The metastable species CO(a³Π) is created by electron-impact reactions



and lost by quenching in the gas phase by the sum of all species, M , by quenching on the walls (W)



and by e-impact ionization



CO($a^3\Pi$) can also be lost by relaxing to the ground state and emitting a photon, but its radiative lifetime is very long (~ 7 ms) [5] hence this destruction pathway is negligible.

The CO($a^3\Pi$) number density is then given by

$$n_{\text{CO}(a)} = \frac{k_7(T_e)n_{\text{CO}}n_e + k_8(T_e)n_{\text{CO}_2}n_e}{k_9n_M + k_{10} + k_{11}(T_e)n_e} \quad (12)$$

where k_i corresponds to the respective reaction equation number.

Electron-impact excitation cross sections have been reported for reactions (1) and (7) [6]. The cross sections for reaction (1) is an estimate [6]. The values for reaction (7) have been reported to be valid, through a fortuitous cancelling of two factor of ~ 10 errors [7]. Unfortunately, no cross sections have been reported for reaction (2). For this optically allowed process, use was made of the cross sections for the optically allowed electron-impact excitation of CO($X^1\Sigma^+$) to the $A^1\Pi$ state, shifted to lower energy by 3.7 eV, the difference in threshold energies for these two processes. Cross sections for reaction (8) have been measured [8]. In that study, a slight ‘upward break’ was observed in the detection of CO($a^3\Pi$) that could have been due to several possible combinations of CO and O states. Attributing the maximum possible signal to this break and all of the effect to the production of CO($b^3\Sigma^+$), an upper limit was obtained for the cross section for reaction (3). Computed cross sections for reaction (11) have also been reported [9].

Gas-phase quenching rate constants, k_9 , for CO($a^3\Pi$) have been measured for a number of species, M , and are generally very fast. For example, CO, H₂, O₂, CO₂, CH₄ have values of 1.1, 2.0, 2.0, 0.2, 3.4, respectively, in units of $10^{-10} \text{ cm}^3 \text{ s}^{-1}$ [10]. The rate coefficient k_{10} for quenching of CO($a^3\Pi$) at the walls is given by [11]

$$1/k_{10} = 1/k_D + 1/k_w \quad (13)$$

where k_D and k_w are rate coefficients for diffusion to and loss at the walls, respectively, given by [12]

$$k_D = \frac{D_{\text{CO}(a)}}{\Lambda_0^2} \quad (14)$$

$$k_w = \frac{\gamma}{2(2-\gamma)} \frac{v_{\text{CO}(a)}A}{V} \quad (15)$$

where $D_{\text{CO}(a)}$ is the binary diffusion coefficient of CO($a^3\Pi$) in the plasma gas mixture. Λ_0 is the characteristic diffusion length for a cylindrical chamber of length L and radius R :

$$\frac{1}{\Lambda_0^2} = \left(\frac{\pi}{L}\right)^2 + \left(\frac{2.405}{R}\right)^2. \quad (16)$$

For $L = 16$ cm and $R = 1.8$ cm, $\Lambda = 0.74$ cm. Given the fast quenching in the gas phase for a variety of species, the value for γ , the probability for quenching upon collision with the walls, was assumed to be unity. $v_{\text{CO}(a)}$ is the mean thermal speed of the metastable, and V and A are the plasma volume and surface area, respectively. For $T = 500$ K and 10 mTorr, the binary diffusion coefficient for CO in H₂ was estimated using

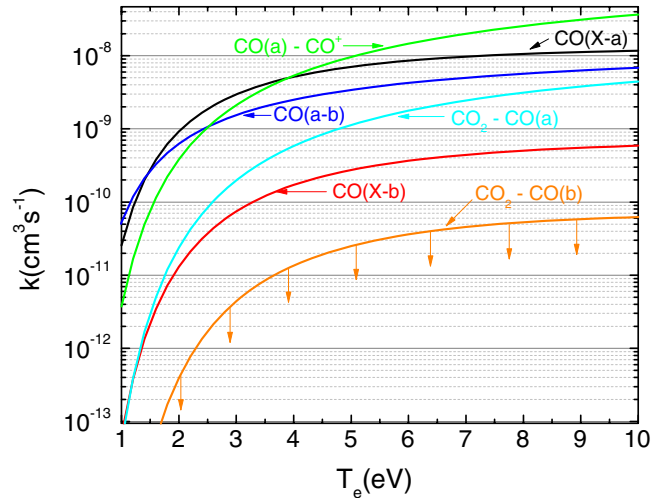


Figure 1. Rate coefficients for relevant electron-impact reactions, computed from published cross sections or upper limits to cross sections, and assuming a Maxwellian electron energy distribution. CO(a)–CO⁺ = reaction (11), CO(X – a) = reaction (7), CO(a – b) = reaction (2), CO₂–CO(a) = reaction (8), CO(X – b) = reaction (1), and CO₂–CO(b) = reaction (3).

equation (17.3-12) of [13] (p 526) to be $1.42 \times 10^5 \text{ cm}^2 \text{ s}^{-1}$. Assuming that the ground state and $a^3\Pi$ state of CO diffuse through the plasma gas mixture and hydrogen at the same rates, $D_{\text{CO}(a)} = 1.42 \times 10^5 \text{ cm}^2 \text{ s}^{-1}$. Hence $k_D = 2.59 \times 10^5 \text{ s}^{-1}$. From equation (15), $k_w = 2.40 \times 10^4 \text{ s}^{-1}$, hence from equation (13), $k_{10} = 2.2 \times 10^4 \text{ s}^{-1}$. It should be noted that uncertainties in the diffusion coefficient estimation should not impact the results since, under these conditions, $k_{10} \sim k_w$.

Using the cross sections given above, rate coefficients computed for the relevant electron-impact reactions are given in figure 1 as a function of T_e . The production of CO emission from dissociative excitation of CO₂ relative to direct excitation of CO from the ground state is simply $k_3n_{\text{CO}_2}/k_{11}n_{\text{CO}}$. It can be shown that, when $n_{\text{CO}_2}/n_{\text{CO}} = 1$, less than 10% of the emission arises from reaction (3), nearly independent of T_e (recall that k_3 is an *upper limit*). We expect $n_{\text{CO}_2}/n_{\text{CO}} < 1$, since the O–CO bond strength is only 5.5 eV and, therefore, should be fragmented by electron impact, while CO, with a bond strength of 11.1 eV, should be hardly dissociated. Furthermore, if CO₂ feed gas is substituted for O₂, emission from CO decreases to undetectable levels at very low powers (e.g. 5 W), while emissions from CO₂⁺ (near 288 nm) and rare gases are still detectable. In CH₃F/O₂ plasmas at higher powers (e.g. 300 W), CO emission is 2 to 3 times more intense than CO₂⁺ emission. Consequently, it is justified to ignore dissociative excitation of CO₂ in the production of CO($b^3\Sigma^+ \rightarrow a^3\Pi$) emission.

For the conditions reported here, T_e varied between 4 and 6 eV. At a pressure of 10 mTorr, using $k_9 = 2 \times 10^{-10} \text{ cm}^3 \text{ s}^{-1}$, $k_{10} = 2.2 \times 10^4 \text{ s}^{-1}$, and the values in figure 1 at $T_e = 5$ eV, $n_{\text{CO}(a)}/n_{\text{CO}}$ ratios were computed using equation (12) as a function of n_e for no CO₂, and for $n_{\text{CO}_2}/n_{\text{CO}} = 1$. In the absence of CO₂, $n_{\text{CO}(a)}/n_{\text{CO}}$ rose linearly with n_e and reached 0.034 at $n_e = 3.5 \times 10^{11} \text{ cm}^3 \text{ s}^{-1}$. A similar linear dependence on n_e was found when $n_{\text{CO}_2}/n_{\text{CO}} = 1$, with a slightly higher

$n_{\text{CO}(a)}/n_{\text{CO}}$ ratio (0.040). Using the $n_{\text{CO}(a)}/n_{\text{CO}}$ ratio with no CO_2 present, 70% of the emission was computed to come from direct excitation of ground state CO and the remaining 30% through the two-step excitation via the $a^3\Pi$ state. With $n_{\text{CO}_2}/n_{\text{CO}} = 1$ these numbers hardly changed (67% and 33%). Therefore the contribution of CO_2 to CO emission through the production of $\text{CO}(a^3\Pi)$ in reaction (8) was ignored.

The CO ($b^3\Sigma^+ \rightarrow a^3\Pi$) emission intensity, I_{CO} , is therefore related to n_{CO} and $n_{\text{CO}(a)}$ by

$$I_{\text{CO}} = I_1 + I_2 = \alpha n_e \sqrt{\frac{2e}{m_e}} \left[n_{\text{CO}} \int_0^\infty \sigma_1(\varepsilon) \varepsilon^{1/2} g_e(\varepsilon) d\varepsilon + n_{\text{CO}(a)} \int_0^\infty \sigma_2(\varepsilon) \varepsilon^{1/2} g_e(\varepsilon) d\varepsilon \right]. \quad (17)$$

Quenching of the $\text{CO}(b^3\Sigma^+)$ can be ignored since its radiative decay rate is much faster than its quenching rate at 10 mTorr. Substituting for $\text{CO}(a^3\Pi)$ number density from equation (12), and neglecting the contribution of CO_2 ,

$$I_{\text{CO}} = \alpha n_e n_{\text{CO}} \sqrt{\frac{2e}{m_e}} \left[\int_0^\infty \sigma_1(\varepsilon) \varepsilon^{1/2} g_e(\varepsilon) d\varepsilon + \frac{k_7(T_e)n_e}{k_9n_M + k_{10} + k_{11}(T_e)n_e} \int_0^\infty \sigma_2(\varepsilon) \varepsilon^{1/2} g_e(\varepsilon) d\varepsilon \right]. \quad (18)$$

The intensity of the $\text{CO}(b^3\Sigma^+ \rightarrow a^3\Pi)$ emission can therefore be expressed as

$$I_{\text{CO}} = \beta(W, P, \dots) n_{\text{CO}} \quad (19)$$

where

$$\beta(W, P, \dots) = \alpha n_e \sqrt{\frac{2e}{m_e}} \left[\int_0^\infty \sigma_1(\varepsilon) \varepsilon^{1/2} g_e(\varepsilon) d\varepsilon + \frac{k_7(T_e)n_e}{k_9n_M + k_{10} + k_{11}(T_e)n_e} \int_0^\infty \sigma_2(\varepsilon) \varepsilon^{1/2} g_e(\varepsilon) d\varepsilon \right] \quad (20)$$

is a factor that depends on plasma conditions (power, pressure, etc) and light detection efficiency.

If CO is added to the plasma, I_{CO} might be expected to rise. $\beta(W, P, \dots)$ can also change with added CO, however. For example, a 2% increase in n_{CO} caused by the addition of a small amount of CO could cause a 1% increase in $\beta(W, P, \dots)$, leading to a 3% increase in I_{CO} . If the same increase in CO caused a 2% decrease in $\beta(W, P, \dots)$, then I_{CO} would not change. Therefore, the effect of CO addition on $\beta(W, P, \dots)$ must be considered. If the addition of a small amount of CO to the feed gas causes a change Δn_{CO} in the CO number density and a change ΔI_{CO} in the CO emission intensity, then a new expression relating emission intensity to CO number density can be written:

$$I_{\text{CO}} + \Delta I_{\text{CO}} = \beta'(W, P, \dots) [n_{\text{CO}} + \Delta n_{\text{CO}}] \quad (21)$$

where $\beta'(W, P, \dots)$ represents a proportionality constant that could be slightly different than $\beta(W, P, \dots)$ because of the effect of adding CO to the plasma. Defining the fractional change in the proportionality constant $a_{\text{CO}} =$

$\beta'(W, P, \dots)/\beta(W, P, \dots)$, and using equations (19) and (21) yields

$$n_{\text{CO}} = \frac{a_{\text{CO}} I_{\text{CO}} \Delta n_{\text{CO}}}{(1 - a_{\text{CO}}) I_{\text{CO}} + \Delta I_{\text{CO}}}. \quad (22)$$

The factor a_{CO} can be determined by making the assumption that the same small change is made in the proportionality constant relating the emission intensity, I_{Ar} , from an inert tracer gas (Ar, at 7504 Å in this work), with a constant number density, n_{Ar} , upon the introduction of a small amount of CO that causes a small change Δn_{CO} in the CO number density and a corresponding small change ΔI_{Ar} in the tracer gas emission intensity, i.e.

$$I_{\text{Ar}} = \chi(W, P, \dots) n_{\text{Ar}} \quad (23)$$

$$I_{\text{Ar}} + \Delta I_{\text{Ar}} = \chi'(W, P, \dots) n_{\text{Ar}} \quad (24)$$

$$(I_{\text{Ar}} + \Delta I_{\text{Ar}})/I_{\text{Ar}} = \chi'(W, P, \dots)/\chi(W, P, \dots) = a_{\text{Ar}} \approx a_{\text{CO}}. \quad (25)$$

The justification for $a_{\text{Ar}} \approx a_{\text{CO}}$ is discussed in the appendix.

There is a possibility that the small perturbation of the plasma caused by the introduction of a small amount of CO might affect differently the excitation of CO emission via the two-step process of reaction (7) followed by reaction (2), than it does the direct excitation of CO in reaction (1). Since (a) the two-step channel accounts for <30% of the emission, (b) the perturbation correction for the two-step process is likely to be similar to the direct excitation process, and (c) the perturbation correction only changes the determined CO number densities by ~20%, ignoring this effect is likely to produce an error of no more than ~5%.

The method of self-actinometry should be more accurate than the 'standard' actinometry method because the change in n_e and $g_e(\varepsilon)$ caused by introducing a trace amount of CO is much less than that caused by varying power, pressure, gas composition, etc over wide ranges. This is also justified in the appendix. In addition, self-actinometry provides *absolute* number densities.

If it is assumed that a small addition of CO does not change the gas conductance for any species or affect the gas temperature, then Δn_{CO} is related to the added CO flow rate, f_{CO} , by

$$\Delta n_{\text{CO}} = n_t \frac{f_{\text{CO}}(1 - \delta)}{f_t} \quad (26)$$

where n_t and f_t are the total number density and total flow rate with CO addition and the plasma on, and δ is the fraction of added CO destroyed by the plasma. Because the feed gases are decomposed by the plasma and form a variety of species including CO, CO_2 , H_2 , H_2O and radicals including H, O, F, CF, etc (not to mention some of the gas that deposits films under some conditions), the total flow rate, summed over all species, is difficult to determine. To circumvent this problem, it is noted that

$$\Delta n_{\text{CO}} = \frac{f_{\text{CO}}(1 - \delta)}{R_g T_g S_{\text{CO}}} \quad (27)$$

where S_{CO} is the effective pumping speed of CO at the reactor exit, R_g is the gas constant and T_g is the gas temperature with

the plasma on. Similarly, the total number density with the plasma off is given by

$$n_t^0 = \frac{f_t^0}{R_g T_g^0 S_{av}^0} \quad (28)$$

where f_t^0 is the total feed gas flow rate, T_g^0 is the gas temperature and S_{av}^0 is the average effective pumping speed of the feed gases, all with the plasma off. Note that the throttle valve position is taken to be unchanged in the above, hence n_t^0 in equation (28) corresponds to the number density at the pressure recorded after the plasma is extinguished (here 10–30% lower than the plasma-on pressure). Since the temperature at the reactor exit does not increase much when the plasma is on, one can assume that the effective pumping speeds do not change much when the plasma is on. Furthermore, the effective pumping speeds of CH₃F, O₂ and CO are nearly the same. Hence setting $S_{CO} \approx S_t^0$, and combining equations (27) and (28) gives a straightforward expression for Δn_{CO} :

$$\Delta n_{CO} = \frac{n_t^0 T_g^0}{T_g} \frac{f_{CO}(1-\delta)}{f_t^0}. \quad (29)$$

It should be pointed out that small errors in Δn_{CO} lead to similar small errors in n_{CO} determined from this self-actinometry method. It should also be noted that one cannot simply establish a small flow of CO with the plasma off and measure the pressure and hence determine Δn_{CO} because this condition corresponds to Knudsen flow, while with all gases flowing and the pressure near 10 mTorr, the flow is transitional and the effective pumping speed is quite different.

Combining equations (22) and (29),

$$n_{CO} = n_t^0 \frac{T_g^0}{T_g} \frac{a_{CO} I_{CO}}{(1-a_{CO})I_{CO} + \Delta I_{CO}} \frac{f_{CO}(1-\delta)}{f_t^0}. \quad (30)$$

Assuming ideal gas behaviour and an accurate measure of pressure P and P^0 with the plasma on and off, respectively,

$$n_t^0 = \frac{P^0}{P} \frac{T_g}{T_g^0} n_t. \quad (31)$$

Therefore, the mole fraction of CO in the plasma, a quantity that does not depend on the difficult-to-determine gas temperature, is given by

$$\frac{n_{CO}}{n_t} = \frac{P^0}{P} \frac{a_{CO} I_{CO}}{(1-a_{CO})I_{CO} + \Delta I_{CO}} \frac{f_{CO}(1-\delta)}{f_t^0}. \quad (32)$$

Equation (32) was used to determine the absolute mole fraction of CO in the plasma. I_{CO} and ΔI_{CO} were measured, while f_{CO} , n_t^0 and f_t^0 were set experimental parameters. The remaining parameters (a_{CO} and δ) were found as shown below.

3.2. Emission intensity measurements and evaluation of parameters a_{CO} and δ

Emission intensities at 296 nm, corresponding to the most intense portion of the (0,1) band of CO($b^3\Sigma^+ \rightarrow a^3\Pi$), were recorded as a function of CO addition to the feed gas

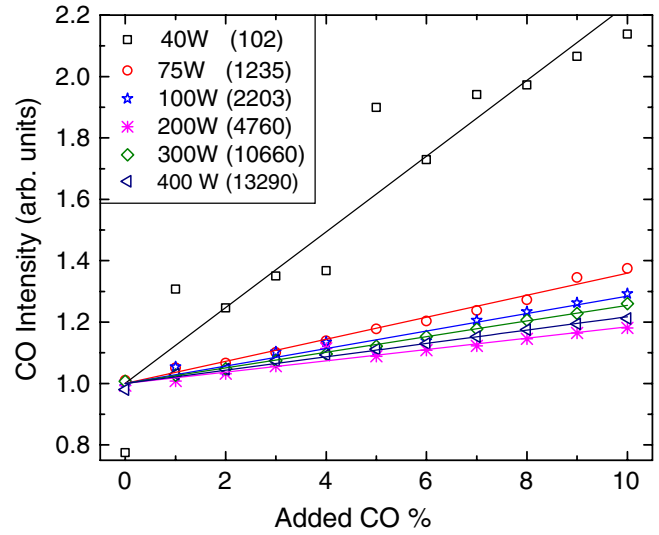


Figure 2. Peak emission intensities of the (0,1) band of CO($b^3\Sigma^+ \rightarrow a^3\Pi$) at 296 nm as a function of CO addition for different plasma powers and fixed throttle valve position. CH₃F and O₂ flow rates were 5 sccm each and the pressure was 10 mTorr (with no CO addition and the plasma on). The raw intensities were normalized to unity at 0% added CO by dividing by the numbers in parentheses. The lines are linear least-squares fits.

for different plasma powers and CH₃F-to-O₂ flow ratios. The power dependence is shown in figure 2. The measurements (points) were normalized to unity at 0% added CO. The relative intensity rises more at low power than at high power because less CO is present from plasma reactions at low power. Between 100 and 400 W, the relative rise in CO emission with added CO seems to saturate (the 200 W data set appears to be an unexplained outlier), suggesting that the reactions forming CO have saturated, or that CO is beginning to be dissociated at higher powers. The data presented below are consistent with the former explanation.

The parameter a_{CO} was assumed to be equal to a_{Ar} (see the appendix). The latter was derived from a plot of the Ar 750.4 nm emission intensity as a function of CO addition at 100 W and equal CH₃F and O₂ feed gas flow rates (4.75 sccm each), shown in figure 3. For this set of experiments, Ar (0.5 sccm) was added while keeping the total flow at 10 sccm with no added CO. From the linear least-squares fit to the 750.4 nm data, the slope/intercept = -0.00790 ± 0.00053 , resulting in $a_{Ar} = 1 - 0.00790 \times (\text{added CO } \%)$. Hence, addition of CO slightly reduced the excitation rate of Ar. The 751.5 nm slope/intercept (absolute) value was somewhat higher, but the agreement between the two lines was reasonable. It was assumed that $a_{Ar} = a_{CO}$ was valid at powers between 75 and 400 W for 50% O₂ addition as well as for O₂ percentages between 20% and 80% at 100 W. Since T_e was found to be nearly independent of power [3] and gas composition [2] for these conditions, this assumption is reasonable.

The fractional dissociation of added CO (δ , defined above) was determined from a plot of $\Delta I_{CO}/I_{Ar}$ versus CO addition as a function of power (figure 4). If any CO was dissociated, then this ratio would decrease with increasing power. No such

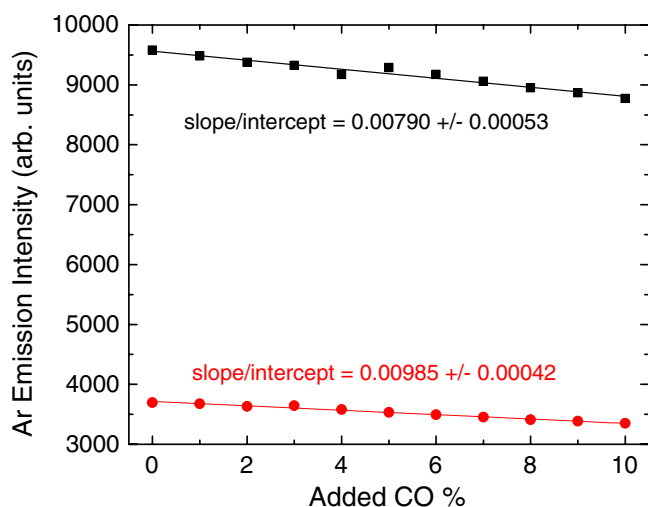


Figure 3. Ar 750.4 and 751.5 nm emission intensities as a function of CO addition. The lines are linear least-squares fits to the measurements. CH₃F, O₂ and Ar flow rates were 4.75 sccm, 4.75 sccm and 0.5 sccm, respectively and the pressure was 10 mTorr (with no CO addition and the plasma on). The slope divided by the intercept for the 750.4 nm line was used to obtain the value for a_{Ar} defined in equation (25).

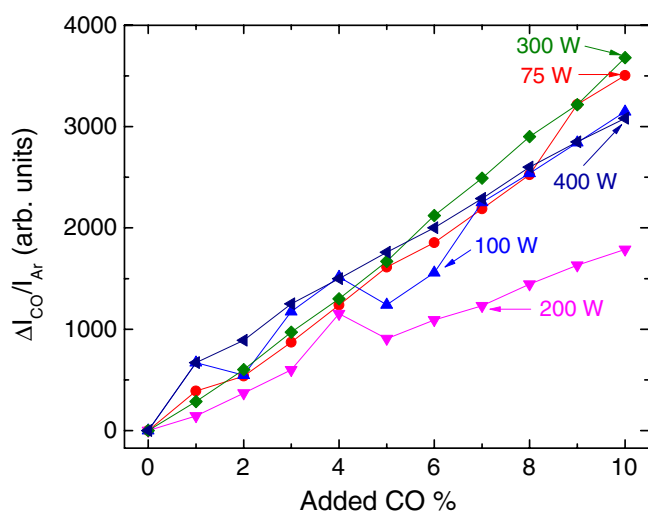


Figure 4. $\Delta I_{CO}/I_{Ar}$ versus CO addition as a function of power, used to show that the fractional dissociation of added CO, δ , is close to zero. CH₃F and O₂ flow rates were 5 sccm each and the pressure was 10 mTorr (with no CO addition and the plasma on).

decrease was observed (excluding the outlying 200 W data), hence very little CO was dissociated by the plasma, as expected, because of the very strong bond energy of CO (11.1 eV). Thus it was assumed that $\delta = 0$ throughout.

3.3. Absolute CO mole fractions determined from self-actinometry and comparisons with relative measurements by actinometry

Absolute CO mole fractions in the plasma (i.e. n_{CO}/n_t) were then determined as a function of power, using equation (32). A plot of n_{CO}/n_t versus added CO is shown in figure 5. n_{CO}/n_t is independent of CO % addition, as would be expected from the

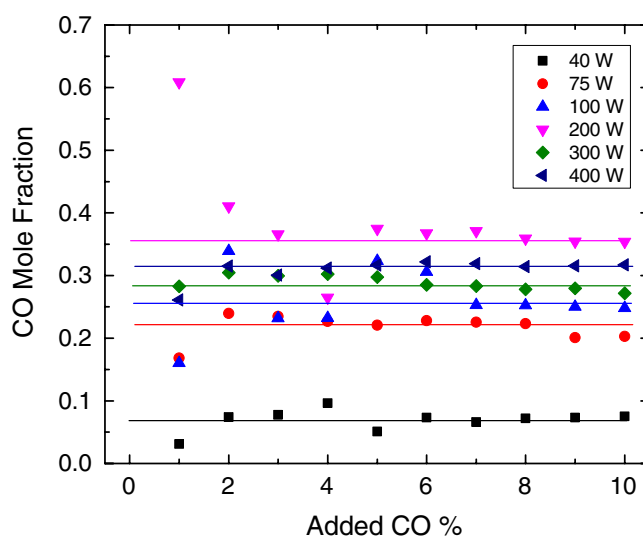


Figure 5. Absolute CO mole fractions in the plasma, n_{CO}/n_t , as a function of added CO at different powers (points). CH₃F and O₂ flow rates were 5 sccm each and the pressure was 10 mTorr (with no CO addition and the plasma on). The line corresponds to the mean values for the points with CO additions between 2% and 10%.

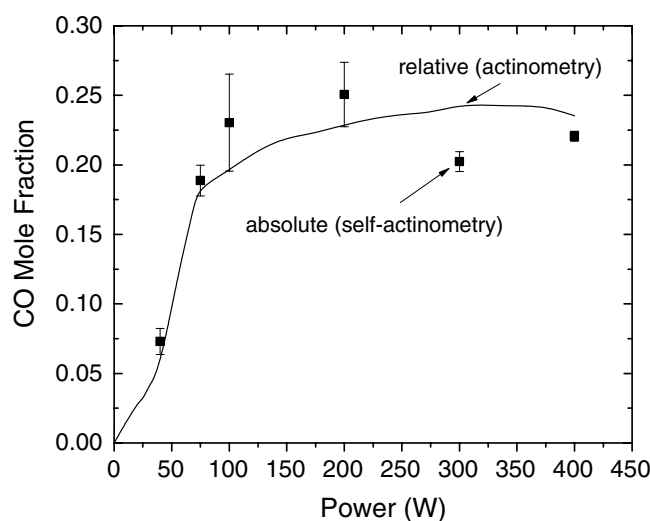


Figure 6. Absolute CO mole fractions in the plasma, n_{CO}/n_t , as a function of power (points). CH₃F and O₂ flow rates were 5 sccm each and the pressure was 10 mTorr (with no CO addition and the plasma on). The error bars are standard errors for the mean values at a given power and CO additions between 2% and 10%. The line corresponds to relative CO-to-Ar number densities derived from measured CO-to-Ar emission intensity ratios in a previous study [2, 3]. (Note: In [3] the flow ratios were incorrectly stated as 1 : 1 : 0.025 in the captions of figures 2–11. The correct value, 0.475 : 0.475 : 0.025, was used to determine all the absolute number densities presented in that study.)

minimally perturbing nature of the measurement. The mean values (from 2–10% CO) are represented by the horizontal lines. Mean values are also plotted as a function of power in figure 6. The error bars represent the standard error of each set of measurements. The CO mole fraction is observed to rise from zero at 0 W power to a near saturated value 0.2–0.25 near 200 W. Since the CH₃F mole fraction in the feed gas was 0.5, this indicates that CO is a major carbon-containing species.

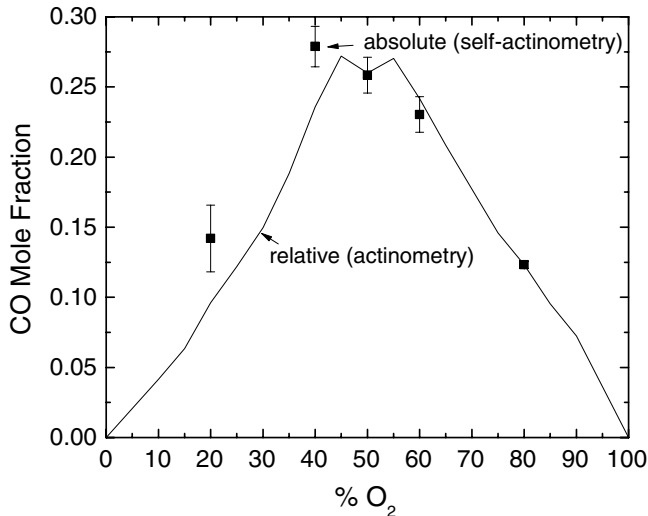


Figure 7. Absolute CO mole fractions in the plasma, n_{CO}/n_t , as a function of %O₂ [= 100 O₂/CH₃F + O₂] in the feed gas ratio (points) at a power of 100 W. CH₃F and O₂ flow rates varied but the total flow rate was 10 sccm and the pressure was 10 mTorr (with no CO addition and the plasma on). The error bars are standard errors for the mean values at a given gas composition and CO additions between 2% and 10%. The line corresponds to relative CO-to-Ar number densities derived from measured CO-to-Ar emission intensity ratios in a previous study [2, 3].

For a constant power of 100 W, the mole fraction of CO went through a maximum value of 0.25 at 50% O₂, as the %O₂ in CH₃F gas was varied (figure 7).

Relative CO mole fractions obtained from the CO-to-Xe 834.7 nm emission intensity ratio (i.e. conventional actinometry) were reported in a previous study [3], and are reproduced in figures 6 and 7, now scaled to the absolute mole fractions determined in the present study. (See the note in the caption of figure 6 concerning the misstated flow rates in [3].) Although the agreement is excellent, it should be pointed out that T_e does not change much as a function of power and gas composition. It is shown in the appendix that CO actinometry will be in serious error for obtaining relative CO number densities under condition where T_e varies substantially, e.g. over a relatively large change in pressure.

3.4. Absolute number densities for major species in CH₃F/O₂ plasmas and overall mass balance

Using the absolute CO mole fractions determined here, absolute number densities for other species determined previously by actinometry [3], and kinetic arguments discussed previously [3], the major species in CH₃F/O₂ plasmas can be given and the overall mass balance can be determined. For the flow rates given above, a pressure of 10 mTorr and a power of 300 W (resulting in a gas temperature of 640 K, as determined previously [3]), the number densities for the major species are given in table 1. Noting that the stoichiometry of the feed gas was C : H : F : O = 1 : 3 : 1 : 2, if it is assumed that nearly all of the carbon is present as CO, then for similar pumping speeds for different species (other than H), the total fluorine number density equals the CO number density. The fluorine

Table 1. Measured species number densities for a 10 mTorr, CH₃F : O₂ : TRG plasma (flow rates of 4.75 : 4.75 : 0.25 sccm, respectively), and 300 W. Under these conditions, no film deposits and the gas temperature is 640 K [3], resulting in a total gas number density of $15.5 \times 10^{13} \text{ cm}^{-3}$.

Species	Number density (10^{13} cm^{-3})
TRG (trace rare gas)	0.36
H	6.5
F	0.79
O	0.72
CO	2.9
Running total of the above species	11.3
Remaining fluorine (assumed HF)	2.1
Remaining oxygen (assumed H ₂ O, OH, CO ₂)	2.2
Running total of all the species	15.6

that is not in the form of F atoms is therefore $(2.9 - 0.8 = 2.1) \times 10^{13} \text{ cm}^{-3}$. We expect most of this fluorine to be present as HF. Similarly, the total oxygen is twice the total carbon, hence the remaining oxygen is $(2 \times 2.9 - 2.9 - 0.7 = 2.2) \times 10^{13} \text{ cm}^{-3}$. This is expected to be mostly in the form of H₂O, OH and CO₂. If all these species are added together, their total number density is $15.6 \times 10^{13} \text{ cm}^{-3}$, which agrees with the value of $15.5 \times 10^{13} \text{ cm}^{-3}$ expected for an ideal gas at 10 mTorr pressure, at a temperature of 640 K.

4. Summary

A ‘self-actinometry’ method based on optical emission spectroscopy was developed to measure the absolute number density of CO in CH₃F/O₂ inductively coupled plasmas. These plasmas are important for selective etching of silicon nitride in the fabrication of FinFET transistors. Keeping the total flow rate of CH₃F and O₂ constant at 10 sccm, a small amount (1–10%) of CO was added to the plasma. This led to a small increase, ΔI_{CO} , in CO($b^3\Sigma^+ \rightarrow a^3\Pi$) emission intensity, as well as a small perturbation in the plasma resulting in a slight decrease in the optical emission intensity of Ar, I_{Ar} , at 750.4 nm as a function of CO addition. Using published cross sections and other kinetics data, it was shown that optical emission arose mainly by electron-impact excitation of ground state CO. Electron-impact excitation out of the CO($a^3\Pi$) metastable state contributed perhaps ~30% of the total emission, while CO emission arising from dissociative excitation of CO₂ made a negligible contribution. Unlike conventional rare-gas actinometry, it was shown that the self-actinometry method is not as prone to errors due to the two-step excitation process through the metastable state, introducing an uncertainty of at most ~5%. At any given CO addition, $\Delta I_{\text{CO}}/I_{\text{Ar}}$ was independent of power, indicating that a negligible amount of CO was dissociated in this plasma.

The absolute CO mole fraction in equimolar mixture (mole fraction 0.5) CH₃F/O₂ feed gas plasmas increased with increasing discharge power to a near saturated value of 0.2–0.25 between 200 and 400 W. Therefore CO was shown to be a major carbon-containing species under these conditions, used in previous studies of CH₃F/O₂ plasmas from this

laboratory [2, 3]. In those studies qualitative optical emission indicated that OH, CO₂, CH, CF and C were also present at what now appears to be smaller concentrations compared to CO. The self-actinometry measurements also indicated that the CO mole fraction as a function of O₂ percentage in CH₃F/O₂ mixtures maximized at 0.25 near 50% O₂. Lastly, actinometric CO-to-Xe relative emission intensity ratios from previous studies [2, 3], when normalized to the absolute mole fractions determined in the present study at one condition, were found to agree over the range of powers and feed gas ratios investigated. This good agreement was likely aided by the fact that T_e was nearly independent of power and gas composition. Using reported electron-impact cross sections, it was shown (see the appendix) that traditional CO actinometry with Xe and particularly Ar will not be a reliable indicator of relative CO number densities when T_e varies substantially. In contrast, the accuracy of self-actinometry is much less affected by changes in T_e .

Acknowledgments

The authors are grateful to Lam Research and the Department of Energy, Office of Fusion Energy Science, contract DE-SC0001939, for financial support of this work.

Appendix

In traditional actinometry, optical emission ratios scale with number density ratios, as well as with electron-impact excitation rate ratios for the species of interest (e.g. CO) relative to the rare gas (e.g. Ar). Excitation rates can change because the electron number density changes, but this does not affect the ratio of excitation rates. Excitation rates are a strong function of the EEDF, especially near threshold energies. Except when the cross sections for the rare gas and the species of interest have the same relative dependence on electron energy at all energies (i.e. the ratio of their cross sections is independent of electron energy), variations in the EEDF can severely limit the accuracy of actinometry, even for relative number density determinations, unless a correction is applied.

The published cross sections for electron-impact excitation from the ground states to excited states of CO($b^3\Sigma^+$) [6], Ar (Paschen 2p₁, emitting at 750.4 nm) [14], and Xe (Paschen 2p₃, 834.7 nm) [15] were used to compute the CO-to-rare gas excitation rate coefficient ratios $k_1(T_e)/k_{Ar}(T_e)$, and $k_1(T_e)/k_{Xe}(T_e)$, plotted in figure A1 as a function of T_e between 1 and 10 eV. The emission intensities of CO and Ar are $I_1 = \alpha n_{CO} n_e k_1$ (see equation (4)) and $I_{Ar} = \alpha n_{Ar} n_e k_{Ar}$, respectively. Thus, if the rate coefficient ratio k_1/k_{Ar} is constant with T_e , then the measured emission intensity ratio will be strictly proportional to the corresponding density ratio (traditional actinometry is valid). However, because the CO excitation threshold is 3 eV lower than that for Ar, the ratio of excitation rate coefficients falls ~10-fold as T_e increases from 1 to 3 eV, and then a further factor of ~3 between $T_e = 3$ and 10 eV. Hence CO relative number density measurements determined by Ar actinometry would be qualitative at best,

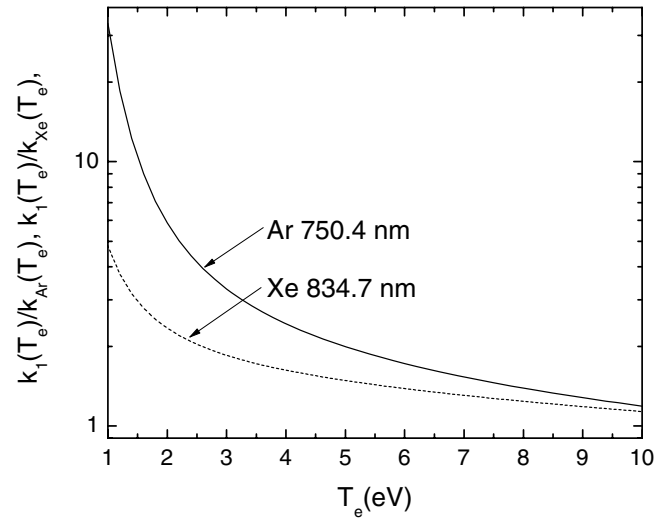


Figure A1. Computed electron-impact excitation rate coefficient ratio for CO emission relative to emission from Ar (2p₁) and Xe (2p₃).

under circumstances where T_e is changing significantly. Using the Xe 834.7 nm line would be better, but would still lead to a substantial error in cases where T_e is changing substantially (e.g. factor of 3 between $T_e = 1$ and 5 eV).

On the other hand, the self-actinometry method is sensitive to the ratio of the *relative* change of the excitation rate coefficients. As with actinometry, n_e cancels out, thus changes in n_e cause no error, but changes in T_e could. The change in the excitation rate coefficient for CO emission, due to a small change ΔT_e in T_e (caused by small additions of CO), relative to the excitation rate coefficient at temperature $T_{e,0}$ (before adding CO) is given by $(1/k_1(T_{e,0}))(dk_1(T_e)/dT_e)\Delta T_e$. The corresponding change for Ar is $(1/k_{Ar}(T_{e,0}))(dk_{Ar}(T_e)/dT_e)\Delta T_e$, where $k_{Ar}(T_e)$ is the electron-impact excitation rate coefficient for Ar 2p₁. The ratio

$$C_f = \left(\frac{1}{k_1(T_e)} \frac{dk_1(T_e)}{dT_e} \right) / \left(\frac{1}{k_{Ar}(T_e)} \frac{dk_{Ar}(T_e)}{dT_e} \right)$$

is a correction factor that should be applied to a_{Ar} (see section 3.2) to recover a_{CO} .

$$a_{CO} = 1 - 0.00790 \times (\text{added CO}\%)$$

$$\times \left(\frac{1}{k_1(T_e)} \frac{dk_1(T_e)}{dT_e} \right) / \left(\frac{1}{k_{Ar}(T_e)} \frac{dk_{Ar}(T_e)}{dT_e} \right). \quad (A1)$$

The correction factor C_f , which represents the relative change in the rate coefficient for direct e-impact excitation of CO (equation (1)), to the relative change in the rate coefficient for direct e-impact excitation of Ar, is plotted as a function of T_e in figure A2. The closer this factor is to unity the better. Since a_{CO} is in both the numerator and denominator of equation (32), using the value of a_{CO} from equation (A1) would increase n_{CO} by only 10%. If it is assumed that half of the observed decrease in Ar emission intensity is due to a small drop in T_e with added CO, then the n_{CO} values should be multiplied by 1.05. This was done for the points in figures 6 and 7. It should also be noted that this small uncertainty could be further reduced by

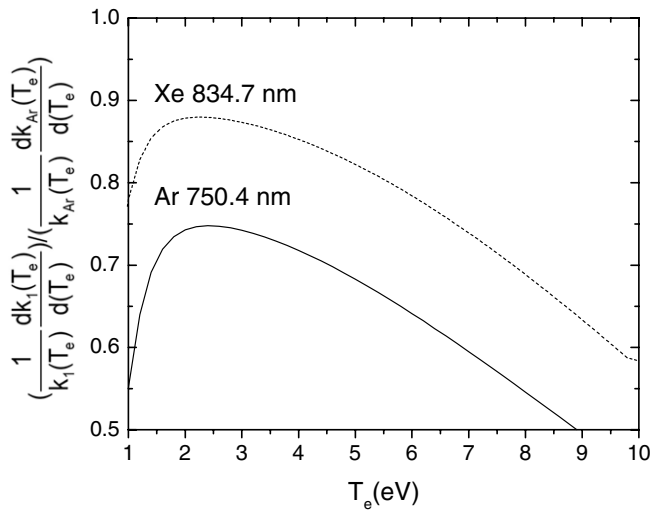


Figure A2. The relative change in computed emission from CO, divided by the relative change in computed emission from Ar ($2p_1$) and Xe ($2p_3$), as a function of electron temperature.

using Xe instead of Ar to sense changes in the perturbation induced by adding CO (dashed curve in figure A2 is closer to unity).

References

- [1] Lee S, Oh J, Lee K and Sohn H 2010 *J. Vac. Sci. Technol. B* **28** 131
- [2] Karakas E, Donnelly V M and Economou D J 2013 *Appl. Phys. Lett.* **102** 034107
- [3] Karakas E, Donnelly V M and Economou D J 2013 *J. Appl. Phys.* **113** 213301
- [4] Kang S J and Donnelly V M 2007 *Plasma Sources Sci. Technol.* **16** 265
- [5] Wauchop T S and Broida H P 1972 *J. Chem. Phys.* **56** 330
- [6] Sawada T, Sellin D L and Green A E S 1972 *J. Geophys. Res.* **77** 4819
- [7] Erdman P W and Zipf E C 1983 *Planet. Space Sci.* **31** 317
- [8] Freund R S 1971 *J. Chem. Phys.* **55** 3569
- [9] Ton-That D and Flannery M R 1977 *Phys. Rev. A* **15** 517
- [10] Taylor G W and Setser D W 1973 *J. Chem. Phys.* **58** 4840
- [11] Xu L, Sadeghi N, Donnelly V M and Economou D J 2007 *J. Appl. Phys.* **101** 013304
- [12] Lieberman M A and Lichtenberg A J 2005 *Principles of Plasma Discharges and Materials Processing* 2nd edn (New York: Wiley)
- [13] Bird R B, Stewart W E and Lightfoot E N 2002 *Transport Phenomena* 2nd edn (New York: Wiley)
- [14] Chilton J E, Boffard J B, Schappe R S and Lin C C 1998 *Phys. Rev. A* **57** 267
- [15] Fons J T and Lin C C 1998 *Phys. Rev. A* **58** 4603